Clays and Clay Minerals, Vol. 60, No. 2, 136–152, 2012.

THE EFFECT OF SMECTITE ON THE CORROSION OF IRON METAL

Barbara A. Balko[1,*], Stephanie A. Bossé[1], Anne E. Cade[1], Elise F. Jones-Landry[1], James E. Amonette[2], and John L. Daschbach[2,3]

[1] Chemistry Department, Lewis & Clark College, Portland, OR 97219 USA
[2] Fundamental and Computational Sciences Directorate, Pacific Northwest National Laboratory, Richland, WA 99352 USA
[3] Environmental Molecular Sciences Laboratory, Pacific Northwest National Laboratory, Richland, WA 99352 USA

Abstract—The combination of zero-valent iron (ZVI) and a clay-type amendment is often observed to have a synergistic effect on the rate of reduction reactions. In the present study, electrochemical techniques were used to determine the mechanism of interaction between the iron (Fe) and smectite clay minerals. Iron electrodes coated with an evaporated smectite suspension (clay-modified iron electrodes, CMIEs) were prepared using five different smectites: SAz-1, SWa-1, STx-1, SWy-1, and SHCa-1. All the smectites were exchanged with Na^{+} and one sample of SWy-1 was also exchanged with Mg^{2+}. Potentiodynamic polarization scans and cyclic voltammograms were taken using the CMIEs and uncoated but passivated Fe electrodes. These electrochemical experiments, along with measurements of the amount of Fe^{2+} and Fe^{3+} sorbed in the smectite coating, suggested that the smectite removed the passive layer of the underlying Fe electrode during the evaporation process. Cyclic voltammograms taken after the CMIEs were biased at the active-passive transition potential for varying amounts of time suggested that the smectite limited growth of a passive layer, preventing passivation. These results are attributed to the Brønsted acidity of the smectite as well as to its ability to sorb Fe cations. Oxides that did form on the surface of the Fe in the presence of the smectite when it was biased anodically were reduced at a different electrochemical potential from those that form on the surface of an uncoated Fe electrode under otherwise similar conditions; this difference suggested that the smectite reacted with the Fe^{2+} formed from the oxidation of the underlying Fe. No significant correlation could be found between the ability of the smectite to remove the Fe passive film and the smectite type. The results have implications for the mixing of sediments and Fe particles in permeable reactive barriers, underground storage of radioactive waste in steel canisters, and the use of smectite supports in preventing aggregation of nano-sized zero-valent iron.

Key Words—Clay Barrier, Fe–Clay Interactions, Fe Corrosion, Montmorillonite, Permeable Reactive Barrier, Smectite, Zero-Valent Iron.

INTRODUCTION

Zero-valent iron (ZVI) (Agrawal and Tratnyek, 1996; Gillham and O'Hannesin, 1994; Gu *et al.*, 1998; Johnson *et al.*, 1996; Matheson and Tratnyek, 1994; Reynolds *et al.*, 1990; Roberts *et al.*, 1996; Tratnyek, 1996) and Fe-bearing clay minerals that have been reduced, typically with dithionite or microbes (Amonette *et al.*, 1996; Cervini-Silva *et al.*, 2000, 2001, 2002, 2003; Hofstetter *et al.*, 2003, 2006; Ilton *et al.*, 2006; Jaisi *et al.*, 2009; Neumann *et al.*, 2008a, 2009, 2012; Nzengung *et al.*, 2001; Peretyazhko *et al.*, 2009; Rodriguez *et al.*, 1999; Schultz and Grundl, 2000), have been studied independently for some time as reductants for certain groundwater contaminants. Not surprisingly, then, the combination of ZVI and clays or clay minerals, including silica, Fe- and non-Fe-bearing and clay-containing sediments, has also been studied as a potential reductant for contaminants (Klausen *et al.*, 2003; Kohn *et al.*, 2003, 2005; Lee *et al.*, 2006; Oh *et al.*, 2007; Powell *et al.*, 1995; Powell and Puls, 1997; Rabideau *et al.*, 1999). In most of these cases, the combination of ZVI and the clay-type amendment had a synergistic effect, resulting in an enhancement of the rate of contaminant degradation. This synergistic effect has been attributed to the ability of clay minerals to maintain the number of active sites on the ZVI surface and to the creation of new reductants in the system.

One property of clay minerals that could allow them to maintain the number of active sites on the ZVI surface is their acidic nature. The Brønsted acidity of clay minerals buffers or even lowers the pH of the ZVI/clay system. Studies by Powell *et al.* (1995) and Oh *et al.* (2007) showed that the addition of clay-containing sediments and silica, respectively, to ZVI resulted in an increase in the rate of Cr^{6+} reduction. In both cases, the authors showed that these amendments served to buffer the system, preventing the typical pH increase that occurs during the reaction in the absence of such additions. Degradation reactions in which ZVI is the reductant have been shown to be sensitive to pH, presumably because the rate of Fe corrosion increases at lower pH, where the passive film is not stable (Matheson and Tratnyek, 1994).

* E-mail address of corresponding author:
balko@lclark.edu
DOI: 10.1346/CCMN.2012.0600204

Clay minerals, however, may also serve to maintain or even increase the number of active sites on the ZVI (and hence the rate of Fe corrosion) because of their ability to sorb products from the oxidation of the ZVI that would otherwise lead to the formation of a passive layer. Rabideau *et al.* (1999) investigated the effect that amending a soil/bentonite slurry wall with ZVI would have on the degradation of trichloroethylene (TCE) and found that the rate constant for the loss of TCE using an Fe/soil/bentonite mixture was 1–2 orders of magnitude greater than using Fe alone. Because Rabideau *et al.* (1999) found that in experiments containing Fe only, the Fe was discolored over the course of their study but no such change was observed when the soil/bentonite mixture was added, the authors attributed some of the increase in degradation rate to the ability of the soil/bentontite mixture to sorb corrosion products. The rate of anaerobic corrosion of steel in bentonite has also been shown, over short times ($\leqslant$1000 h), to be greater than in artificial groundwater at a similar pH (Smart *et al.*, 2004). Analysis of the bentonite showed that products from the Fe corrosion were transported into the clay, which would limit the formation of a passivation layer. In a later study, Carlson *et al.* (2007) used several different analytical techniques to examine what happened to the Fe ions when steel or cast iron corroded over a long time period (356–911 days) in bentonite. When bentonite was present, the corrosion layer was less voluminous than in its absence. Mössbauer analysis of the clay showed an increase in the Fe^{2+}/Fe^{3+} ratio. Some of the Fe^{2+} produced by the corroding Fe appeared to exchange with the interlayer Na^{+} in the clay. Carlson *et al.* (2007) explained their Mössbauer results by the reduction of structural Fe(III) in the bentonite through the exposure to Fe or that some of the Fe^{2+} from the corroding Fe entered the octahedral sheets.

Clay minerals may also be able to sorb products which do not contain Fe from degradation reactions involving ZVI that would otherwise block active sites on the Fe. The effect of amorphous silica and silica sand on the rate of reduction of Cr^{6+} by ZVI was studied by Oh *et al.* (2007). They found that while both materials increased the rate of removal of Cr^{6+} relative to ZVI alone, the amorphous silica had a greater effect. Because of the presence of Cr on the silica surfaces, the authors attributed the effect of the amendments to the ability of both silica and sand to sorb the Cr^{3+} reaction products; the silica had a greater effect because of its larger surface area and its ability to form stronger surface complexes with Cr^{3+} than the sand. The authors recognized, however, that the ability of silica to buffer the pH of the system, which the sand cannot do, may have contributed also.

Another explanation for the reducing capability of ZVI and clays together is that the combination produces additional reducing agents in the system, namely structural Fe(II), sorbed Fe^{2+}, and $H\cdot$ or $H_2(g)$. Clay minerals reduced by dithionite and/or microbes have been used successfully to reduce nitroaromatics (Hofstetter *et al.*, 2003, 2006; Neumann *et al.*, 2008b), chloropicrin (trichloronitromethane) (Cervini-Silva *et al.*, 2000), various chlorinated aliphatic compounds (Amonette *et al.*, 1996; Cervini-Silva *et al.*, 2001, 2002, 2003; Neumann *et al.*, 2009; Nzengung *et al.*, 2001; Rodriguez *et al.*, 1999), and radionuclidies (Ilton *et al.*, 2006; Jaisi *et al.*, 2009; Peretyazhko *et al.*, 2009); the reducing ability is generally attributed to the reduction of structural Fe(III) to Fe(II) by the dithionite or microbes. The ZVI or sorbed Fe^{2+} from the corrosion of the ZVI could act analogously to dithionite or microbes (Amonette, 2002; Merola *et al.*, 2007; Schaefer *et al.*, 2011), reducing the structural Fe(III) in the clay mineral. Another new reductant in the system could be the Fe^{2+} from the corrosion of the Fe that sorbs to the clay mineral. Past studies have suggested that sorbed Fe^{2+} is capable of reducing certain compounds, most notably nitroaromatics (Schultz and Grundl, 2000). Because sorbed Fe^{2+} is capable of reducing structural Fe(III), however (Schaefer *et al.*, 2011), the actual reductant may be structural Fe(II). Powell *et al.* (1995) and Powell and Puls (1997) believed that the protons generated by the dissolution of clay minerals could also serve as electron acceptors, allowing the formation of other potential reductants (*e.g.* Fe^{2+}, $H\cdot$, and $H_2(g)$).

Some studies, however, have found that the combination of ZVI and a clay-type amendment have led to a decrease in the rate of contaminant reduction (Cervini-Silva *et al.*, 2002; Klausen *et al.*, 2003; Kohn *et al.*, 2003, 2005). Typically in these studies, the loss in performance was attributed to the clay blocking active sites on the ZVI rather than ensuring that these active sites remain available. For example, batch and column studies (Klausen *et al.*, 2003; Kohn *et al.*, 2003, 2005) have shown that the addition of dissolved silica to the ZVI/contaminant system resulted in a decrease in the rate of contaminant reduction. In these cases, the silica acted as a corrosion inhibitor, presumably because a silica overlayer formed on the Fe surface, preventing the oxidation of the ZVI and consequently the reduction of the contaminant. In another study, Cervini-Silva *et al.* (2002) investigated how the combination of ZVI and SWa-1 affected the rate of degradation of pentachloroethane. The fastest rates were obtained with dithionite-reduced SWa-1. The rates were much slower for ZVI alone and even slower using unreduced SWa-1 alone. When a combination of ZVI and SWa-1 (either dithionite-reduced or unreduced) was used as the reductant, however, the rate constant for the dechlorination was only slightly greater for the unreduced SWa-1 alone when using the reduced SWa-1/ZVI and essentially the same as the unreduced SWa-1 when using the unreduced SWa-1/ZVI. The results suggest that the ZVI somehow adversely affected the redox properties of the clay mineral and that the clay mineral limited the

https://doi.org/10.1346/CCMN.2012.0600204 Published online by Cambridge University Press

degradation reaction due to the Fe alone, presumably by blocking active sites on the Fe surface through complexation and precipitation reactions.

In the present study, details of the interaction between one of the most important types of clay mineral in temperate soils, smectite, and ZVI were examined electrochemically. Passivated Fe electrodes that were coated with smectite (so-called clay-modified iron electrodes or CMIEs) following a method developed by Bard and Mallouk (1992) and Fitch (1990) were prepared. These electrodes were then studied using two electrochemical techniques: potentiodynamic polarization scans (PPSs) and cyclic voltammetry. As the smectite coating on the CMIEs is not electrically connected to the underlying Fe electrode, the electrochemical behavior of the CMIE is expected to be the same as that of an uncoated, passivated Fe electrode, except for the effect that the smectite has on the Fe. From the PPSs, the corrosion potential (E_{CORR}), the primary passive potential (E_{PP}), the critical anodic current (I_C), and the current in the passive region (I_{PASS}) were obtained. Comparing these values with those from an uncoated, passivated Fe electrode, made it possible to determine how effective smectites are at removing the passive layer on Fe, enhancing corrosion of Fe, and limiting further growth of the oxide layer at the Fe surface. Three regions in the cyclic voltammograms (CVs) were used to determine how the smectite changed the corrosion of the underlying Fe electrode: the Fe oxidation peak that represents the transition between active and passive behavior, the anodic peaks that are associated with further oxidation of the Fe(II) oxides in the passive layer, and the corresponding reduction peaks for these oxides. The height and position of these peaks indicated the extent of the oxide layer on the Fe surface and allowed the authors to determine whether the Fe^{2+} that was produced during the corrosion of Fe was sorbed into the smectite or remained at the Fe−smectite interface where it would subsequently be oxidized and then reduced. Also, the potential at which the reduction peaks occurred indicated how the oxides that formed in the presence of the smectite when the Fe electrode was biased anodically differed from those formed in the absence of the smectite coating. The CVs recorded after biasing the CMIE at E_{PP} were used to determine whether the smectite film could remove Fe oxides that formed on the Fe surface during the biasing. Seven different smectites were used with a range of surface areas, cation exchange capacities (CEC), and Fe contents, as well as two different exchange cations, to allow determination of how specific smectite properties affected the smectite–Fe interaction. The information obtained from these electrochemical studies suggested ways to maximize the reactivity for the smectite-Fe combination and also limitations to the use of ZVI in field settings where smectite may be present in the soil. The results should also be considered in plans for storage of nuclear waste, which typically involves storage of the waste in stainless steel containers and steel overpacks that are surrounded by bentonite or smectite-containing rock (Féron *et al.*, 2008; Madsen, 1998).

MATERIALS AND METHODS

Materials

Smectites. Five different smectite-dominated clays were obtained from the Source Clays Repository of The Clay Minerals Society. The smectites used were a hectorite from California (SHCa-1), three montmorillonites (SAz-1, SWy-1, and STx-1), and a ferruginous smectite (SWa-1).

Smectite processing. The clays were processed to isolate the smectite fraction following a method developed by one of the authors (JEA) that is based on procedures described by Jackson and others (Tanner and Jackson, 1948; Jackson *et al.*, 1950; Jackson, 1979). The clays were first fractionated to obtain particles <2 μm in size. A 5% suspension of the clay in a pH 9.5, 0.0375 M Na_2CO_3 solution was shaken overnight on a reciprocating platform shaker to disperse the particles. The next day, the sand-sized particles were removed by wet-sieving through a 63 μm sieve. The <2 μm clay particles were separated from the silt-sized particles remaining in the suspension by gravitational sedimentation. In order to concentrate the smectite suspension, a 5 M $MgCl_2$ solution was added to flocculate the clay; the suspension was then centrifuged (Sorvall RC 3B Plus with a H-6000A swinging-bucket rotor) for 20−30 min at 2000 rpm (≈1150 g) and the clay that settled recovered. The concentrated smectite suspensions were then Na-saturated and acid washed to remove carbonates. To do this, the Mg-saturated smectite suspension was centrifuged (Beckman GS-15 with F0850 fixed-angle rotor) for 15 min at 5000 rpm (≈2700 g). The supernatant was removed and a 0.001 M HCl/1 M NaCl solution (HCl was ACS Reagent grade; the NaCl was from Aldrich, 99+%) was added to the remaining smectite. The smectite was re-suspended and then centrifuged again. The supernatant was removed and the pH measured. The re-suspension/centrifugation procedure was repeated until the pH was equal to that of the 0.001 M HCl/1 M NaCl solution (pH ≈ 3). Then a solution of 0.1 M NaCl was added to the smectite. This smectite suspension was then centrifuged, the supernatant removed, and the pH of the supernatant measured. The re-suspension/centrifugation process was repeated until the pH of the suspension reached ~5.6 (the pH of the 0.1 M NaCl solution). A sample of SWy-1, after it had been exchanged with Na^+ cations, was exchanged with Mg^{2+} cations. To do this, a sample of SWy-1 was re-suspended with 1 M $MgCl_2$. The suspension was shaken for 45 min and then centrifuged for 15 min. The smectite fraction was again re-suspended with the 1 M $MgCl_2$ and shaken overnight. The suspension was then centrifuged

https://doi.org/10.1346/CCMN.2012.0600204 Published online by Cambridge University Press

and re-suspended with 0.1 M $MgCl_2$. After centrifugation, the smectite fraction was re-suspended with 0.01 M $MgCl_2$. After shaking and centrifuging the smectite again, it was re-suspended with deionized (DI) water. After processing the smectites, the excess chloride ions were removed. First, an ultrasonic homogenizer (Cole Parmer 4710 Series, Chicago, Illinois, USA) with a 5 mm diameter tip was placed in the smectite suspension and energized for ~30 min to disperse the colloids. The smectite suspensions were then put in dialysis tubing (Spectra/Por 7, Spectrum Laboratories, Inc.) and the tubing soaked in DI water, which was replaced regularly. When the conductivity of the water was <0.6 μmho cm^{-1}, the smectite suspensions were freeze-dried (Labconco Freezone 12) and stored until use.

Electrochemical cell. The electrochemical experiments were carried out using a nylon, custom-fabricated, three-electrode electrochemical cell with a volume of ~4 mL. The working electrode, the CMIE, was sealed onto the back of the cell; the front of the cell had a glass window that allowed the authors to monitor the CMIE visually. The counter electrode was a platinum wire coil (EG&G, Princeton Applied Research RDE0021, Oak Ridge, Tennessee, USA), and the reference electrode was a saturated calomel electrode (SCE) (EG&G, Princeton Applied Research K0077). A bridge tube allowed the positioning of the reference electrode within millimeters of the CMIE. All voltages are reported with respect to the SCE. The electrolyte used was pH 8.4 borate buffer prepared from 0.0375 M $Na_2B_4O_7{\cdot}10H_2O$ (Aldrich Chemical Company, ACS reagent grade) and 0.15 M H_3BO_3 (Aldrich Chemical Company, 99.5+% analytical grade reagent). The buffer was purged for at least 30 min with Ar gas (99.998%, Polar Cryogenics Specialty Gases, Portland, Oregon, USA) before it was added to the cell.

Fe electrode. The Fe working electrodes used in the experiments were made from Fe rod with a diameter of 12 mm (99.99% pure from Alfa Aesar Ward Hill, Massachusetts, USA). As all the electrodes used had the same diameter; current rather than current density is reported. To prepare the electrodes for use, a stainlesss steel wire was welded to the Fe and then the piece encased in epoxy (Struers, Epofix resin and hardner, Cleveland, Ohio, USA). The electrode surface was exposed and the underlying Fe polished roughly using a progression of 250 to 600 grit silicon carbide polishing paper (carbimet discs; Buehler, Lake Bluff, Illinois, USA). Prior to each experimental run, the Fe electrode was polished using 600 and/or 800 grit silicon carbide paper followed by a suspension of 1-μm deagglomerated alpha alumina (Al_2O_3), which was applied to a nylon or microcloth polishing disc (Buehler, Lake Bluff, Illinois, USA). The electrode was washed with a 2% soap solution (Micro-90, International Products Corporation, Burlington, New Jersey, USA) and rinsed with DI water between polishes. Once a mirror-like surface was achieved, the electrode was rinsed and then sonicated (Branson, model 2210, Danbury, Connecticut, USA) for 5 min to remove any alumina residue. Finally, the electrode was dried with a Kimwipe™ (Irving, Texas, USA) and rinsed with methanol (99.9% ACS spectrophotometric grade; Sigma-Aldrich, St. Louis, Missouri, USA). The Fe electrodes were typically polished and then left in air for 60 min before any electrochemical experiments or coating with smectite. The polished Fe electrodes used could be expected to have a passive layer on their surface. A passive layer was found (Deng *et al*. 2004, 2006) to have developed on an Fe surface within minutes of air exposure and grew slowly over time.

Clay-modified iron electrodes. The CMIEs were prepared by evaporating a smectite suspension on the polished Fe electrodes, following the method developed by Fitch (1990) and Bard and Mallouk (1992). A 0.10−0.15 mL aliquot of a smectite suspension (10 g/L to 20 g/L), which was prepared from the freeze-dried, processed smectite, was pipetted onto the center of the electrode and the suspension spread out to cover most of the electrode surface. As the underlying Fe electrode was passivated, any small fraction of the Fe electrode that remained uncoated would not contribute significantly to the electrochemical measurements. The coated Fe electrode was kept in a desiccator (plastic, BelArt, Wayne, New Jersey, USA) that was evacuated (Welsh Dry Pressure Vacuum Pump 2545B01, Niles, Illinois, USA) and then filled with N_2 gas (99.998%, Liquid Carbonic Specialty Gases, Slatersville, Rhode Island, USA) during the evaporation. The smectite suspension required ~45 min to dry. The desiccator was purged with N_2 gas and re-evacuated every 15 min during this drying time to maintain an O_2-free environment, which was necessary to keep the Fe from rusting. When the smectite suspension was fully dry, the desiccator was vented with N_2 gas and then the electrode removed and immediately screwed into the back of the electrochemical cell.

The smectite coating remained intact during the electrochemical experiments. No evidence of any significant dissolution of the film was found. Occasionally during experiments the swollen smectite film would slide off the underlying Fe electrode in one intact piece; this would be immediately apparent in changes in the electrochemical signal and visual inspection of the electrode (data from experiments in which the smectite film slid off were disregarded).

Measurement of total Fe sorbed to SAz-1. A modification of the Gibbs' method (Gibbs, 1979) was used to measure the amount of Fe that sorbed into the smectite film during the preparation of the SAz-1 CMIEs. After appropriate exposure to the Fe electrode during drying, the smectite film was removed using a flexible rubber

https://doi.org/10.1346/CCMN.2012.0600204 Published online by Cambridge University Press

scraper attached to a glass rod (*i.e.* a rubber policeman (Jensen, 2008)). The smectite film was shaken briefly in a solution of 5 M HCl (prepared by diluting concentrated HCl (Ashland, ACS reagent, Covington, Kentucky, USA)) and then soaked for 20 min. During the soaking time, the smectite settled. A sample of the supernatant was removed, placed in a glass cuvet, and the pH adjusted to between 4 and 6 using 1 M NaOH. This was necessary because the formation of the colorimetric indicator complex, *i.e.* Fe^{2+}-ferrozine, required a sample pH between 4 and 6 (Gibbs, 1979; Stookey, 1970). The reductant (hydroxylamine hydrogen chloride $NH_2OH{\cdot}HCl$ (Aldrich, 98%, ACS reagent)) was then added and the mixture was allowed to stand for 2 min. Finally, the ferrozine reagent (made using ferrozine (3-(2 pyridyl)-5,6-diphenyl-1,2,4-triazine-p, p′-disulfonic acid, monosodium salt (Aldrich, 97%), and 5 M HCl), sodium acetate buffer (prepared from $CH_3CO_2Na{\cdot}3H_2O$ (Aldrich, 99%, ACS reagent)), and acetic acid (prepared from glacial acetic acid, Mallinckrodt, analytical, St. Louis, Missouri, USA)) were added. After 20 min, the peak height at 562 nm was measured using a UV/VIS spectrophotometer (HP 8452A diode array). A calibration curve was made using a solution of ferrous ammonium sulfate ($Fe(NH_4)_2(SO_4){\cdot}6H_2O$ (Aldrich, 99%, ACS reagent)) in 5 M HCl.

To ensure that the Fe detected came from sorbed Fe rather than structural Fe, the ferrozine test was also performed using the SAz-1 suspension rather than the smectite film that had been removed from the Fe electrode. No significant amount of Fe was detected from the SAz-1 suspension, suggesting that the smectites did not dissolve under the extraction conditions used. Note, however, that the moles of Fe detected by this method may underestimate the actual amount of Fe sorbed as all of it may not have been extracted.

Experimental

Electrochemistry. An EG&G Princeton Applied Research model 273A potentiostat on loan from Pacific Northwest National Laboratory was used for the CV experiments and a Versastat II potentiostat (Princeton Applied Research, PowerCorr software) was used for the PPSs. In both cases, the 590 Hz electronic filter was used. The uncoated electrodes and CMIEs were allowed to stabilize for 20 min, unbiased in the borate buffer, before a PPS or CV was run. The stabilization time was chosen to ensure that the smectite film was in equilibrium with the aqueous solution. Soaking a smectite-coated electrode in the supporting electrolyte for 5 min is regarded as sufficient to establish the interlayer spacing of the smectite (Joo and Fitch, 1996). Note that the Fe electrodes (uncoated or coated) were not reduced prior to scanning. The open-circuit potential (OCP) of the electrode was recorded during the stabilization time as this measurement was found to be a good indicator of the quality of the smectite attachment. The OCP for the polished uncoated Fe electrode was ~−0.31 V and for the CMIE, ~−0.74 V. These values did not change significantly during the stabilization period.

The PPSs generally were started at a potential of ~0.2 V cathodic of the initial OCP of the electrode to prevent oxidation of the Fe electrode and scanned in the anodic direction at a potential of at least 0.3 V anodic of the OCP. The scan rate was 0.166 mV/s. Typical scans ranged from ~−1.0 V to −0.4 V. E_{CORR}, the corrosion potential, was taken to be the minimum in the logarithmic plot of absolute current *vs.* potential and the uncertainty in this measurement was taken as the standard deviation (σ_{xn-1}) for the experiments carried out. The corrosion current could not be determined reliably from the PPS plots because of the small linear region and the variability in the shape of the PPS as separate anodic and cathodic scans were not recorded. What was more useful was to compare the following three parameters for the CMIE with those for the uncoated Fe electrode: (1) the primary passive potential, E_{PP}, which is the potential at which the active-to-passive transition occurs; this was taken as the potential at which the peak current occurred in the region of the PPS at potentials anodic of the corrosion potential; (2) the log of the critical anodic current, I_C, which is the current at E_{PP}; and (3) I_{PASS}, the current in the passive region (−0.4 V for the CMIE and −0.2 V for the bare Fe electrodes).

The typical CV was recorded from −0.9 V to 0.0 V and back to −0.9 V at a scan rate of 5 or 10 mV/s. Only the first scan was recorded. The CVs were also recorded after biasing the CMIE at −0.6 V_{SCE}, which is $\approx E_{PP}$, for times ranging from 0 to 20 min. In these biasing experiments, the electrodes were left at the OCP after biasing so that the total time (time at the OCP plus time at the bias potential) that the electrode was held in solution prior to the CV would still be 20 min. At −0.6 V_{SCE}, the Fe metal was expected to oxidize to Fe(II) and gradually form an hydroxide layer ($Fe(OH)_2$), which is the start of the passivation (Babić *et al.*, 2003; Büchler *et al.*, 1998; Diez-Perez *et al.*, 2001; Jovancicevic *et al.*, 1987; Scherer *et al.*, 1997; Vela *et al.*, 1986). As is shown below, the smectite coating removes the passive film from the Fe electrode during the drying process; the present biasing experiments will show whether the smectite can remove a passive film formed *in situ*. If the smectite can remove the *in situ* passive film, biasing at −0.6 V_{SCE} should have no effect on the CVs; however, if the smectite cannot remove the *in situ* passive film, the CV would approach that of a passivated Fe electrode as the biasing time increased.

Comparison was made between potentials measured in these electrochemistry experiments, which are referenced to the saturated calomel electrode, and others referenced to a saturated KCl, AgCl/Ag reference electrode. In these cases, 0.045 V was subtracted from

https://doi.org/10.1346/CCMN.2012.0600204 Published online by Cambridge University Press

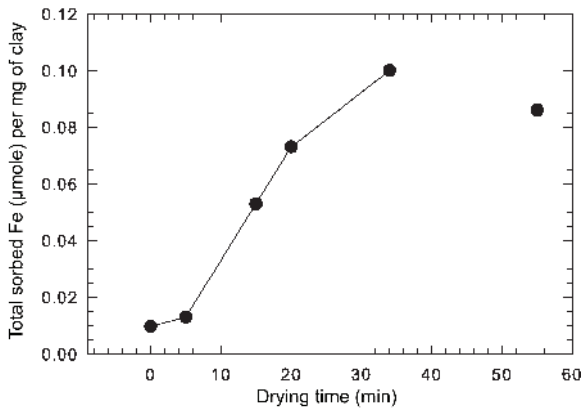

Figure 1. Amount of Fe sorbed on the SAz-1 smectite film (μmole/mg) during preparation of the clay-modified Fe electrodes. Line added for clarity only. The point at 0 min drying time was achieved using the SAz-1 suspension before it was applied to the Fe electrode. The point at 55 min of drying time was recorded after the electrode had been soaked in borate buffer for 5 min.

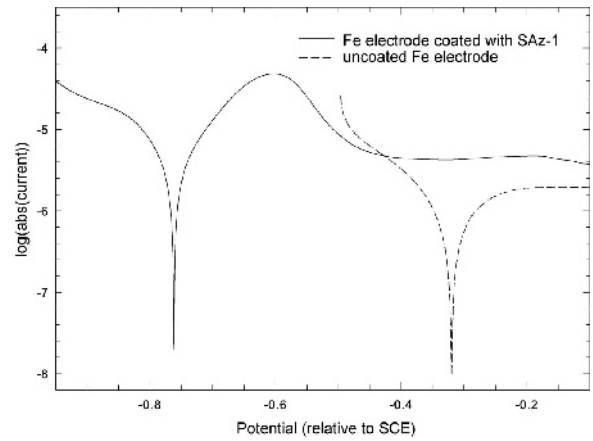

Figure 2. Representative potentiodynamic polarization scans (log absolute current in amperes *vs.* potential) for an Fe electrode coated with SAz-1 (solid line) and an uncoated Fe electrode (dashed line). The scan rate was 0.166 mV/s. The scans were carried out in de-aerated borate buffer, pH 8.4. E_{CORR}, E_{PP}, log(I_C), and I_{PASS} for the electrodes were determined from the potentiodynamic polarization scans.

the latter measurements to allow comparison of results (Sawyer *et al.*, 1995).

RESULTS

Total Fe sorbed to SAz-1.

The total amount of Fe that sorbed into the SAz-1 coating during the 45 min drying process increased as the smectite coating dried on the underlying Fe electrode (Figure 1). This result suggests that corrosion of the underlying Fe electrode and/or the passive layer occurred during the drying process and that the Fe^{2+} and Fe^{3+} cations produced were sorbed by the smectite.

Potentiodynamic polarization scans

Values for E_{CORR}, E_{PP}, log(I_C), and I_{PASS} were determined from the PPSs taken using the Fe electrodes coated with all the Na^+-exchanged smectites as well as an uncoated Fe electrode (Figure 2, Table 1). No critical point was observed at potentials anodic of E_{CORR} in the case of the uncoated Fe electrodes, indicating that the uncoated Fe electrode was passivated as expected (Research, 1987). This assessment was confirmed by the E_{CORR} for the uncoated electrodes which was characteristic of E_{CORR} of Fe with an air-formed passive film in a pH 8.4 borate buffer solution. The OCP of freshly polished electrodes that had been exposed to dry air for various amounts of time was measured in a previous study (Deng *et al*., 2004, 2006). Those authors found that the OCP, which is equivalent to E_{CORR}, went from ~−0.7 V_{SCE} after exposure for ~2 min to ~−0.3 V_{SCE} after exposure for ~190 min. The measured OCP continued to increase to ~−0.14 V_{SCE} after ~2000 min of

Table 1. Average of parameters from potentiodynamic polarization scans for the uncoated iron electrode and iron electrodes coated with Na^+-exchanged smectites. The uncertainty is taken as the standard deviation (σ_{xn-1}) for the experiments performed. The number of experiments (n) used to determine the average and standard deviation is included. Data from all of the smectites is averaged in the 'all smectites' column.

	Uncoated	SAz -1	STx-1	SWa-1	SWy-1	SHCa-1	All smectites
E_{CORR} (V)	−0.31±0.01	−0.77±0.01	−0.74±0.03	−0.74±0.03	−0.72±0.03	−0.71±0.03	−0.74±0.03
E_{PP} (V)	NA	−0.62±0.01	−0.61±0.02	−0.616±0.004	−0.600±0.001	−0.602±0.008 (n = 4)	−0.61±0.01 (n = 23)
Log (I_c)	NA	−4.44±0.07	−4.5±0.1	−4.7±0.3	−4.7±0.2	−4.55±0.04 (n = 4)	−4.5±0.2 (n = 23)
I_{PASS} (μA)	1.7±0.2 (at 0.2 V)	3.6±1.5 (n = 5) (at 0.4 V)	2.9±0.7 (at 0.4 V)	3±1 (n = 3) (at 0.4 V)	1.145±0.007 (n = 2) (at 0.4 V)	2±1 (n = 3) (at 0.4 V)	3±1 (n = 19) (at 0.4 V)
n	3	6	6	4	3	5	24

https://doi.org/10.1346/CCMN.2012.0600204 Published online by Cambridge University Press

exposure. The changes in the OCP observed by Deng *et al.* (2004, 2006) were associated with an increase in the thickness of the passive layer.

In contrast to the E_{CORR} of the uncoated Fe electrode, the overall E_{CORR} for the CMIEs, which combines data from all the smectites, is typical of that of a freshly reduced Fe electrode with a minimal amount of oxide present (Table 1). The E_{CORR} values for freshly reduced Fe in N_2-free pH 8.4 borate buffer have been reported in the literature as -0.765 V_{SCE} (-0.72 $V_{Ag/AgCl}$) (Nurmi *et al.*, 2004; Scherer *et al.*, 1997) and -0.80 V_{SCE} (Deng *et al.*, 2006) The presence of varying amounts of oxide on the Fe and different Fe electrode geometries have both been shown to decrease the magnitude of E_{CORR} slightly from these values. Exposure to dry air for even a few minutes was observed (Deng *et al.*, 2006) to change the OCP of their freshly reduced Fe electrodes from -0.80 V_{SCE} to -0.70 V_{SCE}. The E_{CORR} for powder disk electrodes (PDEs) (Nurmi *et al.*, 2004) was ~-0.745 V_{SCE} (-0.70 $V_{Ag/AgCl}$). Nurmi *et al.* (2004) believed that E_{CORR} for their PDEs was slightly more positive than E_{CORR} for a freshly reduced Fe electrode because of the physical differences in microstructure, dislocations, defects, and surface oxides in their electrodes. That the magnitude of the overall E_{CORR} for the CMIEs was slightly less than that of a freshly reduced Fe electrode suggests that either the removal of the passive layer by the smectite coating was not entirely complete or that the presence of the smectite film caused subtle alterations in the physical environment around the Fe electrode.

Comparing the critical anodic current from the CMIE PPSs with those found by Nurmi *et al.* (2004) for their PDEs suggested a mechanism whereby the smectite is able to maintain an oxide-free Fe surface. The CMIE has a prominent active-passive transition (*i.e.* a large critical anodic current) (Figure 2, Table 1). By comparison, the stationary Fe PDEs of Nurmi *et al.* (2004) showed almost no active-passive transition peak, though that peak in the Nurmi *et al.* (2004) Fe PDEs appeared and grew in prominence as the rate of rotation of their electrode was increased. This transition peak in the Nurmi *et al.* (2004) study showed an increase in current that was linear with the square root of rotation rate, suggesting that the reactions in the active-passive transition (the dissolution of Fe and the formation of the passive film) were controlled by mass transport. Those authors surmised that the mass-transport limitation found with Fe PDEs was related to the difficulty in transporting Fe^{2+} out of the pores in their PDEs; when the Fe^{2+} built up near the Fe-particle surfaces at low rotation rates, the corrosion rate decreased as did the critical anodic current observed in the PPS (Nurmi *et al.*, 2004). Even though the CMIEs were stationary, the small critical anodic current/mass-transport limitation seen by Nurmi *et al.* (2004) for their stationary electrodes was not seen, presumably because the Fe^{2+} produced in the corrosion was sorbed readily into the smectite film and did not have the opportunity to accumulate on the Fe-electrode surface.

While the PPSs clearly showed a difference between the uncoated Fe electrodes and CMIEs, the difference in behavior for CMIEs prepared with the different smectites studied was less obvious (Table 1). The degrees of uncertainty in E_{CORR}, E_{PP}, $\log(I_C)$, and I_{PASS}, estimated as the standard deviation, make it difficult to determine whether a correlation exists between any of these electrochemical parameters and smectite properties (Table 2). The E_{CORR} for the electrode coated with SAz-1 is significantly different from the electrode coated with SWy-1 and SHCa-1 (an upper limit of -0.76 V for SAz-1 *vs.* a lower limit of -0.75 V for SWy-1 and -0.74 V for SHCa-1). As discussed, the more oxide on an Fe electrode, the greater the difference from -0.8 V. Thus, the comparison of E_{CORR} values suggests that the electrode coated with SAz-1 was marginally less passivated or more active than electrodes coated with SWy-1 or SHCa-1. The smectite properties for which SAz-1 is on one extreme and SWy-1 and SHCa-1 are on the other are CEC, surface area, and perhaps surface pH, although insufficient data were available for this last property. The percentage of Fe(II) or Fe(III) in the smectite and the tetrahedral, octahedral, or interlayer charge, however, do not correlate with the trend in E_{CORR}.

Comparison of the E_{CORR} values for the uncoated Fe electrode and the CMIEs suggests that the smectite film removed most of the passive layer on the Fe electrode. Based on the measurements of the Fe^{2+} and Fe^{3+} sorbed into the smectite coating during the drying process, the removal occurred while the smectite suspension dried on the Fe electrode. Continued contact between the smectite coating and underlying Fe electrode, however, was necessary to prevent the build-up of a significant passive layer during the electrochemical experiments when the electrode was biased anodically. During one of the PPS scans of a CMIE coated with SWa-1, the smectite film slipped off (Figure 3). Before running the scan (after the initial 20 min stabilization), the OCP of the electrode was typical of that of a CMIE (-0.76 V_{SCE}). After the smectite film slipped off (at ~-0.7 V_{SCE}) the scan was allowed to continue and minima (E_{CORR}) were observed at ~-0.50 and at ~-0.34 V_{SCE}. The second minimum at -0.34 V_{SCE} agreed with E_{CORR} for the uncoated, air-passivated electrode and suggests that the same type of passive film ultimately formed on this electrode. The minimum at -0.50 V may be due to the formation of an intermediate Fe oxide on the electrode surface. Anodic polarization voltammograms for Fe_3O_4 and Fe_2O_3 powder disk electrodes taken by Nurmi *et al.* (2004) showed E_{CORR} values in this range: ~-0.465 V_{SCE} for $Fe(0)/Fe_2O_3$ (-0.42 $V_{Ag/AgCl}$) and ~-0.625 V_{SCE} for $Fe(0)/Fe_3O_4$ (-0.58 $V_{Ag/AgCl}$) (Nurmi *et al.*, 2005). The minimum may also be an artifact due to the current

https://doi.org/10.1346/CCMN.2012.0600204 Published online by Cambridge University Press

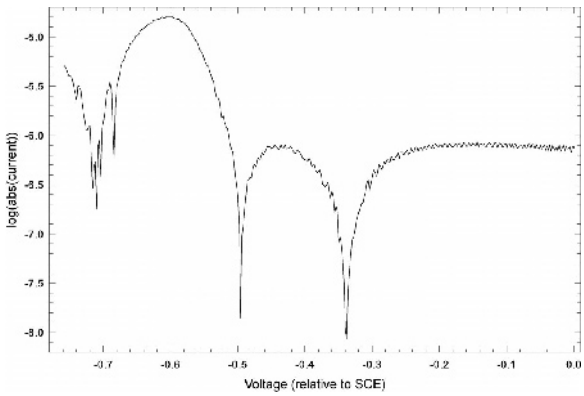

Figure 3. Potentiodynamic polarization scan (log absolute current in amperes *vs.* potential) of an Fe electrode coated with SWa-1 from −0.8 V_{SCE} to 0.0 V_{SCE} in de-aerated borate buffer, pH 8.4. The scan rate was 0.166 mV/s. At ~ −0.7 V_{SCE} the smectite film slipped off.

going from positive to negative during the formation of the passive layer on the Fe surface.

Cyclic voltammograms

Cyclic voltammograms were taken for a CMIE electrode coated with SAz-1 and an uncoated Fe electrode, both held at the OCP prior to the scan, and an uncoated Fe electrode that was reduced for 15 min at −0.9 V_{SCE} to remove some of the passive layer before the scan. The peaks in these CVs were compared to those that typically appear in CVs of freshly reduced Fe electrodes in de-aerated pH 8.4 borate buffer (Figure 4). The CV for the uncoated Fe electrode that was not reduced prior to the sweep was virtually featureless compared to CVs of freshly reduced Fe electrodes from the literature (Büchler *et al.*, 1998; Diez-Perez *et al.*, 2001; Jovancicevic *et al.*, 1987; Oblonsky and Devine, 1995; Scherer *et al.*, 1997; Vela *et al.*, 1986), confirming that the uncoated electrode had a passive layer. When the uncoated electrode was held at −0.9 V_{SCE} prior to the scan, however, the peaks expected for the Fe electrode began to emerge, as the biasing removed oxides. The CV from the electrode coated with SAz-1, however, had several of the same peaks typically found in CVs from freshly reduced Fe, despite the fact that the electrode was not reduced prior to the scan. Oxidation peak I was the most prominent feature. Oxidation peak I in the literature (~−0.55 to −0.60 V_{SCE}) is usually attributed to the oxidation of the Fe metal to Fe(II) and formation of an hydroxide layer ($Fe(OH)_2$) (Babić *et al.*, 2003; Büchler *et al.*, 1998; Diez-Perez *et al.*, 2001; Jovancicevic *et al.*, 1987; Scherer *et al.*, 1997; Vela *et al.*, 1986). This peak represents the transition between active and passive behavior as the hydroxide layer that develops slows further dissolution of the Fe.

At potentials anodic of oxidation peak I is a small bump that probably indicates oxidation peak II′, which was seen by others (includng Babić *et al.*, 2003; Büchler *et al.*, 1998; Diez-Perez *et al.*, 2001) at ~ −0.2 V_{SCE} for an Fe electrode under certain experimental conditions. Lowering the pH (Diez-Perez *et al.*, 2001) or multiple cycling (Babić *et al.*, 2003; Büchler *et al.*, 1998; Diez-Perez *et al.*, 2001) enhances this peak as does use of an

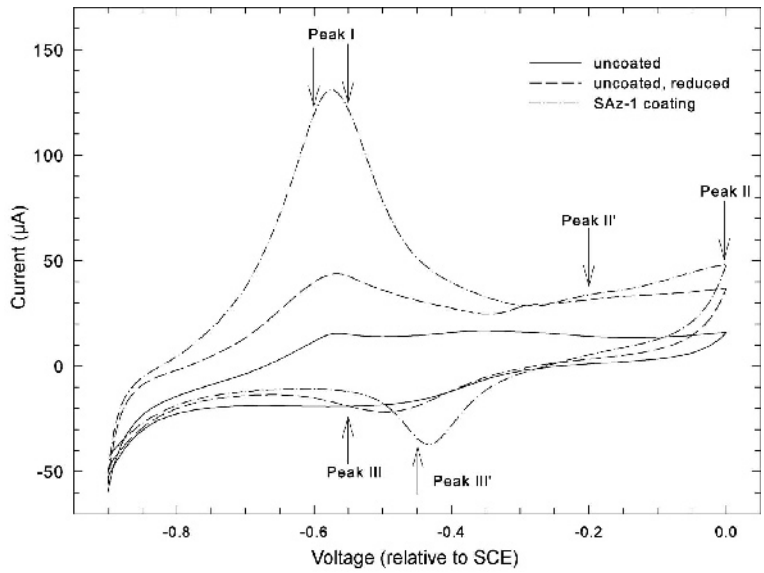

Figure 4. Cyclic voltammograms (current *vs.* potential plot) taken for unreduced, uncoated Fe electrode (solid line); uncoated Fe electrode that was held at −0.9 V for 15 min prior to the scan (dashed line); and Fe electrode coated with 0.15 mL of 10 g/L SAz-1 (dash-dot line) in de-areated borate buffer (pH 8.4). The scan was from −0.9 V_{SCE} to 0 V_{SCE} to −0.9 V_{SCE} at a scan rate of 10 mV/s. The arrows show where oxidation and reduction peaks typically occur for freshly reduced Fe electrodes in an anaerobic pH 8.4 borate buffer.

https://doi.org/10.1346/CCMN.2012.0600204 Published online by Cambridge University Press

electrochemical cell with only a small amount of electrolyte in front of the electrode (Büchler *et al.*, 1998). The peak is suggested (Büchler *et al.*, 1998) to be due to the oxidation of the aqueous Fe^{2+} present at the electrode surface and the formation of an outer porous hydroxide deposit layer, such as FeOOH or $Fe(OH)_3$, that does not inhibit the formation of an inner passive film. Thus, this peak is expected under conditions when Fe^{2+} accumulates at the electrode surface.

Oxidation peak II is commonly seen at potentials anodic of oxidation peak I and typically appears as a broad peak that occurs at ~0.0 V_{SCE} (Babić *et al.*, 2003; Diez-Perez *et al.*, 2001). The CMIE CV, however, showed only a hint of this peak in that the current increased at the end of anodic sweep. When the anodic scanning limit was extended positive of 0.0 V_{SCE}, only a broad increase in current was observed, not a well defined peak (data not shown). In the literature, oxidation peak II is typically attributed to the oxidation of the Fe(II) oxide/hydroxide layer formed at ~−0.55 to −0.60 V (peak I) to an Fe(II)/Fe(III) oxide film (probably Fe_3O_4/Fe_2O_3).

The CMIE CVs (Figure 4) showed a reduction peak at ~−0.45 to −0.40 V_{SCE}. This probably corresponds to reduction peak III′ seen in the literature under certain experimental conditions (Büchler *et al.*, 1998; Diez-Perez *et al.*, 2001) as it is the reduction peak corresponding to oxidation peak II′. This peak typically occurs at ~−0.45 V_{SCE} and is believed to be due to the reduction of the outer Fe(III) hydroxide deposit layer (Babić *et al.*, 2003; Büchler *et al.*, 1998; Diez-Perez *et al.*, 2001). The reduction peak seen with the CMIE is significantly anodic of reduction peak III that is observed with a freshly reduced, uncoated Fe electrode (~−0.55 V_{SCE}). Reduction peak III corresponds to the oxidation peak II and is associated with the cathodic reduction of the Fe(III) species in the inner passive film to aqueous Fe^{2+} or $Fe(OH)_2$ (Babić *et al.*, 2003; Büchler *et al.*, 1998; Jovancicevic *et al.*, 1987).

The difference in the position of the reduction peak for the CMIE and the reduced, uncoated Fe electrode (Figure 4) suggests that the oxides that formed at the Fe surface on the CMIE were different from those which formed on the reduced, uncoated Fe. A different oxide layer might form in the presence of the smectite for several reasons. First, the presence of the smectite coating may change the hydrodynamics of the system, encouraging the formation of the oxides that are associated with peaks II′ and III′. Note that peaks II′ and III′ are often found when an electrochemical cell with only a small amount of electrolyte in front of the electrode is used, presumably because of the oxidation of aqueous Fe^{2+} trapped at the electrode surface to form an outer hydroxide deposit layer and the corresponding reduction of this layer (Büchler *et al.*, 1998). While the smectite may sorb some of the Fe^{2+} from the electrode surface, it may also change the hydrodynamics at the electrode surface, effectively trapping any remaining Fe^{2+}, which could then be oxidized. A second explanation for why different oxides form in the presence of smectite may, instead, be due to the removal of Fe^{2+} by the smectite. For example, the passive film that forms in the presence of EDTA, which complexes with Fe^{2+}, was found to be different from that formed in the absence of EDTA; in the presence of EDTA, the passive film was thinner, had a higher donor (oxygen vacancies) concentration, and lacked an outer Fe_2O_3 layer (Liu and Macdonald, 2001; Sikora and Macdonald, 2000). Third, the oxides formed in the presence of the smectite may differ from those formed on an uncoated Fe electrode because of reactions between the smectite and Fe^{2+}. The presence of montmorillonite, for example, has been shown to alter the precipitation products of aqueous Fe^{2+}

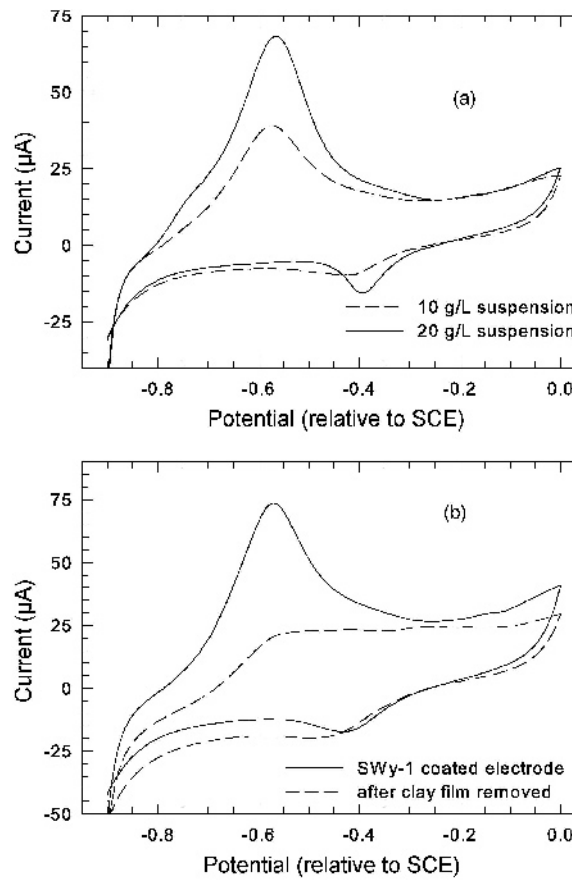

Figure 5. Cyclic voltammograms showing the effect of the amount of smectite used. In the experiments shown, the scans were carried out in a de-areated borate buffer (pH 8.4) from −0.9 V_{SCE} to 0 V_{SCE} to −0.9 V_{SCE}. (a) SWa-1 coated Fe electrode prepared using 0.10 mL of a 20 g/L smectite suspension (solid line) *vs.* a 10 g/L smectite suspension (dashed line). The scan rate was 5 mV/s. (b) SWy-1 coated Fe electrode prepared using 0.15 mL of a 10 g/L smectite suspension (solid line) *vs.* the same electrode after the smectite coating was wiped away in air (dashed line). The scan rate was 10 mV/s.

https://doi.org/10.1346/CCMN.2012.0600204 Published online by Cambridge University Press

(Krishnamurti *et al.*, 1998). At pH 6.0, the presence of the montmorillonite blocked the formation of goethite and maghemite and favored the formation of ferrihydrite, while at pH 8.0, the presence of montmorillonite blocked the formation of maghemite and goethite and favored the formation of lepidocrocite. A possible mechanism for the interaction between the smectite and Fe^{2+} is electron transfer to the structural Fe(III) in the smectite. For example, in solutions of aqueous Fe^{2+}, electron transfer between the sorbed Fe^{2+} species and structural Fe(III) ions in the smectite was found to promote the formation of Fe(III)-(hydr)oxides, which in turn led to the precipitation of Fe^{2+} in the form of mixed oxidation state (green rust) compounds (Thompson and Mitchell, 1993).

The changes in the CV associated with the smectite coating were strongly dependent on the amount of smectite in the film. The CVs for a CMIE coated with 0.10 mL of a 10 *vs.* a 20 g/L suspension of SWa-1 showed changes in the heights of the oxidation and reduction peaks; the more smectite present in the film, the greater the height of the peaks associated with the presence of the smectite (Figure 5a). When the smectite film was removed by wiping the CMIE with a Kimwipe™ in air, the CV scan reverted to that typical of a passivated Fe electrode (Figure 5b).

The CVs for CMIEs prepared with different smectites were compared to determine whether a correlation existed between specific smectite properties and the electrochemical behavior of the electrodes (Figure 6). These CVs were taken within days of each other to minimize experimental variability. The trend in the height of peak I with smectite type showed the same trend seen in E_{CORR}. Peak I, indicative of the activity of Fe, was largest in the CV for the CMIE prepared from SAz-1, while it was smallest in the CVs for CMIEs prepared from SWy-1 and SHCa-1. The uncertainty in the individual CVs, however, was too large to carry out a meaningful correlation analysis between the height of peak I and specific smectite properties.

One consistent difference in the CVs taken using CMIEs prepared with different smectites is the position of the reduction peak (peak III′) (Figure 6). When SWa-1 was used as the coating, the reduction peak always appeared at a more positive potential (−0.40 *vs.* −0.44 V_{SCE}) than when the other smectites were used, supporting the explanation that different oxides form in the presence of the smectites because of electron-transfer reactions between sorbed Fe^{2+} and structural Fe(III) in the smectite. Because SWa-1 has significantly more structural Fe(III) than any of the other smectites used (Table 2), an SWa-1 coating would be expected to have the greatest effect on the oxide formed if this mechanism were correct. A change in the height of this reduction peak would not necessarily be expected as the formation of the oxides would be limited by the amount of Fe^{2+} sorbed. The current associated with the electron transfer from the structural Fe(III) to the sorbed Fe^{2+} would not be expected to appear in the CV because the smectite is isolated electrically from the Fe electrode.

To investigate the effect that the exchange cation had on the interaction of the smectite and Fe, CVs for SWy-1 exchanged with Na^+ and with Mg^{2+} were compared (Figure 7). Peak I was much greater when the Mg^{2+}-exchanged smectite was used. The difference in CVs suggested that the CMIE with the Mg^{2+}-exchanged

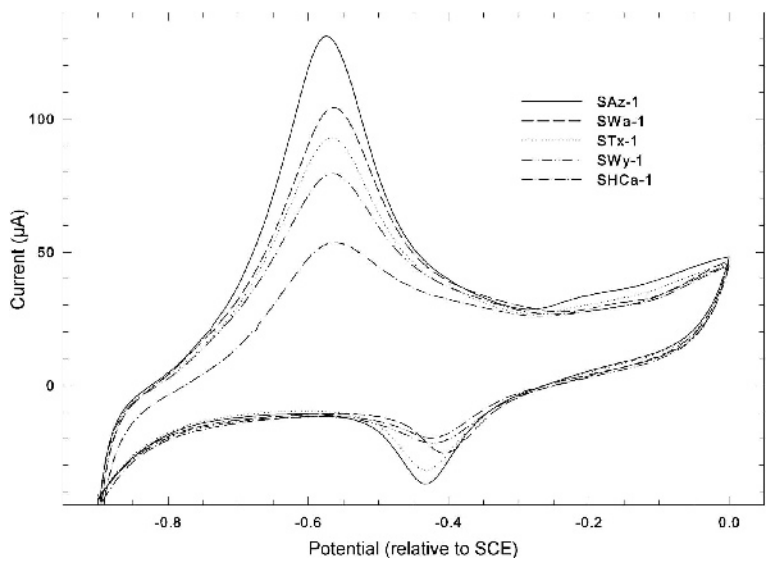

Figure 6. Cyclic voltammograms (current *vs.* potential plot) taken for Fe electrodes coated with five different types of smectites. For each type of smectite, 0.15 mL of a 10 g/L suspension was used to form the coating. The scans were carried out in de-areated borate buffer (pH 8.4) from −0.9 V_{SCE} to 0 V_{SCE} to −0.9 V_{SCE} at a scan rate of 10 mV/s.

https://doi.org/10.1346/CCMN.2012.0600204 Published online by Cambridge University Press

Table 2. Properties of smectites used in the present experiments.

	SAz-1	STx-1	SWa-1	SWy-1	SHCa-1
CEC (meq/100 g)	120	84	107[a]	77	44
SA from BET analysis (m^2/g)	97	84	36[b]	32	63
SA from glycol sorption (m^2/g)	820	599	662	720[e]	486
Initial pH	6.8[c]				10.3[c]
% Fe(III) as Fe_2O_3	1.42	0.65	25.25[d]	3.35	0.02
% Fe(II) as FeO	0.08	0.14	0[d]	0.32	0.25
Octahedral charge	−1.08	−0.68	−0.18[d]	−0.53	−1.35
Tetrahedral charge	0.0	0.00	−0.91[d]	−0.02	−0.22
Interlayer charge	−1.08	−0.68	−1.09[d]	−0.55	−1.57

All values were taken from van Olphen and Fripiat (1979) with the following exceptions: [a] Zen *et al.* (1996); [b] Schultz and Grundl (2000); [c] Rabideau *et al.* (1999); [d] Source Clay Physical/Chemical Data (2011); [e] Lear and Stucki (1989).

smectite was more active than the Na^+-exchanged smectite, presumably because more of the passive layer was removed by the Mg^{2+}-exchanged smectite during the drying process. In addition, the current in the CV associated with the oxidation of Fe(II) in the passive layer was significantly greater for the Mg^{2+}-exchanged smectite. This suggests that when Mg^{2+} was the exchange cation, much of the excess Fe^{2+} produced during the active-passive transition was not sorbed into the smectite but was oxidized instead. This may have been because more Fe^{2+} was produced and/or because it is more difficult for the Fe^{2+} to exchange with Mg^{2+} than with Na^+. These possibilities are discussed in the next section. Although the oxidation current was greater for the Mg^{2+}-exchanged smectite, no corresponding change in reduction current in the return sweep was observed, suggesting that the additional oxides that formed were somehow removed by the smectite before the return sweep.

The measurement of sorbed Fe in the clay film during the preparation of the CMIEs and the appearance of the CMIE CVs suggest that the smectite film removed the air-formed passive layer from the Fe electrode while the smectite suspension was evaporated onto the Fe electrode. Could the smectite film, however, remove oxides that were formed in the presence of the smectite in the borate buffer electrolyte? To investigate this question, CVs were recorded after biasing the CMIE at −0.6 V_{SCE}, the potential of the active-passive transition, for varying amounts of time. During the biasing time, the Fe was expected to be oxidized to Fe(II) and form an Fe hydroxide layer ($Fe(OH)_2$) (Babić *et al.*, 2003; Büchler *et al.*, 1998; Diez-Perez *et al.*, 2001; Jovancicevic *et al.*, 1987; Scherer *et al.*, 1997; Vela *et al.*, 1986).

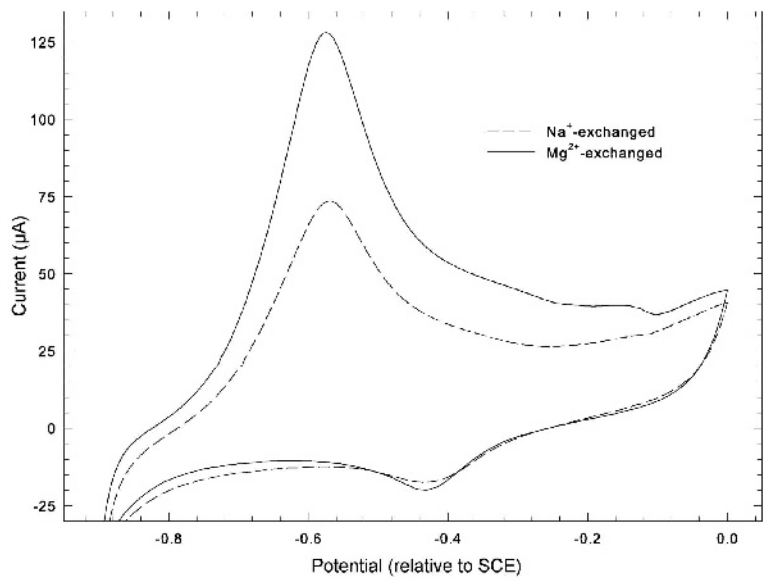

Figure 7. Cyclic voltammograms (current *vs.* potential plot) taken for Fe electrodes coated with Na^+-exchanged SWy-1 (dashed line) and Mg^{2+}-exchanged SWy-1 (solid line). In both cases, the films were prepared using 0.15 mL of a 10 g/L smectite suspension. The scans were carried out in de-areated borate buffer (pH 8.4) from −0.9 V_{SCE} to 0 V_{SCE} to −0.9 V_{SCE} at a scan rate of 10 mV/s.

https://doi.org/10.1346/CCMN.2012.0600204 Published online by Cambridge University Press

Biasing the CMIE at −0.6 V_{SCE} for as little as 5 min caused a slight decrease in the height of peak I (Figure 8); additional time at −0.6 V_{SCE}, however, led to no further decreases. Presumably, peak I decreased when the CMIE was biased at −0.6 V_{SCE} because some Fe oxides/hydroxides formed on the Fe surface, beneath the smectite coating, during the biasing. Note, however, that not enough Fe oxides formed during the biasing to passivate the Fe electrode; if the electrode were passivated, peaks I and III′, which were prominent, would not be present. These results suggest that the smectite was able to remove most of the Fe(II) oxides/hydroxides generated during the biasing at the active-passive transition. The CVs taken after biasing at −0.6 V_{SCE} also showed a small increase in current at potentials associated with oxidation peaks II′ and II, probably due to the oxidation of the Fe^{2+} that was generated during active-passive transition but not sorbed into the smectite. Reduction peak III′ also increased, probably because of the reduction of the additional oxides formed during the biasing and subsequent anodic sweep.

DISCUSSION

Removal of passive layer

Comparison of the PPSs and CVs taken using uncoated Fe electrodes with those taken using the CMIEs shows that the smectite film removed the air-formed passive layer on the Fe electrodes. Measurements of the sorbed Fe in the smectite films during the preparation of the CMIEs suggested that this removal occurred when the smectite film was evaporated onto the Fe electrode. The biasing experiments showed that the smectite film was able to remove an oxide/hydroxide layer formed in the presence of the smectite in the borate buffer solution. The most likely mechanism responsible for the removal of the passive film both during the evaporation of the suspension and in solution is acidic dissolution. Reductive dissolution may also play a role, however, especially for the oxide/hydroxide layers formed at the active-passive transition.

Chemical dissolution by an acid. The rate of dissolution of passive films on Fe (Bardwell *et al.*, 1988) as well as Fe oxide films (Virtanen *et al.*, 1997) has been shown to increase with increasing solution acidity. This pH dependence can be explained, at least in part, by dissolution reactions such as (Virtanen *et al.*, 1997):

$$Fe_2O_3 + 6H^+ \rightarrow 2Fe^{3+}(aq) + 3H_2O$$
$$Fe_3O_4 + 8H^+ \rightarrow 2Fe^{3+}(aq) + Fe^{2+}(aq) + 4H_2O.$$

Smectites are Brønsted acids due primarily to the dissociation of water that is polarized by the smectite's exchangeable cations (Adams *et al.*, 1983; Frenkel, 1974; Mortland and Raman, 1968; Wei *et al.*, 2001). As isomorphic substitution in the octahedral sheets causes stronger acidity than in tetrahedral sheets (Frenkel, 1974; Mortland and Raman, 1968; Wei *et al.*, 2001), the smectites used in the present study are expected to be more acidic than other types of clay minerals. Because smectites are proton donors, the presence of the smectite could cause any Fe oxides on the Fe surface to dissolve, especially during the evaporation of the smectite suspension on the Fe surface. The more dehydrated the smectite, the more acidic it will be (Adams *et al.*, 1983; Frenkel, 1974; Mortland and Raman, 1968; Soma and

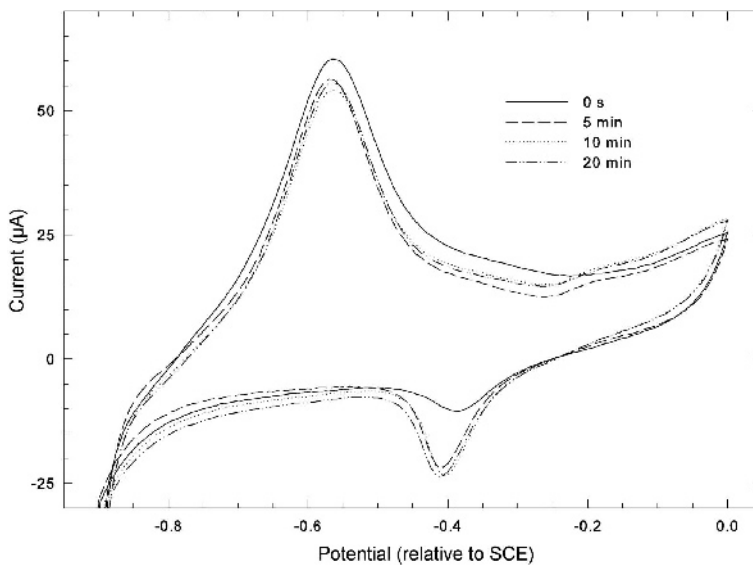

Figure 8. Cyclic voltammograms (current *vs*. potential plot) taken for Fe electrodes coated with SWa-1 (0.1 mL of a 20 g/L suspension). 0.15 mL of a 10 g/L smectite suspension was used to form the coating. The scans were carried out in de-areated borate buffer (pH 8.4) from −0.9 V_{SCE} to 0 V_{SCE} to −0.9 V_{SCE} at a scan rate of 5 mV/s. The electrodes were held at −0.6 V_{SCE} for varying amounts of time prior to the CV sweep. The total stabilization time in all cases remained at 20 min.

https://doi.org/10.1346/CCMN.2012.0600204 Published online by Cambridge University Press

Soma, 1989) because the Brønsted acidity of the smectite is primarily derived from the water polarized by the exchangeable cations. Dissolution of the passive film during the preparation of the CMIE was, therefore, not unexpected.

The acidity of the smectite would also be expected to depend on the ability of the exchangeable cations to polarize water. Thus, smectites exchanged with small, highly charged cations are most acidic (Frenkel, 1974; Mortland and Raman, 1968). The Mg^{2+}-exchanged smectite would be expected to be more acidic than the corresponding Na^{+}-exchanged smectite and so the Fe surface of the CMIE exchanged with Mg^{2+} should have fewer oxides than the Fe surface of the CMIE exchanged with Na^{+}, explaining why peak I in the CV of the CMIE prepared with the Mg^{2+}-exchanged smectite was greater than in the CV of the CMIE prepared with the Na^{+}-exchanged smectite (Figure 7). The appearance of greater current in the Mg^{2+}-exchanged CMIE CV anodic of peak I also suggested that more Fe oxides formed at the surface of the Fe electrode during the anodic sweep, perhaps because the ability of the smectite to sorb all of the Fe^{2+} produced was overwhelmed. While this was probably due to some degree to the increased production of Fe^{2+}, a difference in the ability of the Mg^{2+}-exchanged smectite to sorb Fe^{2+}may also have some role and would be especially true if some of the Fe^{2+} were sorbed by the smectite through cation exchange, as displacement of Mg^{2+} by Fe^{2+} would be expected to be more difficult than displacement of Na^{+} by Fe^{2+}. Despite the increase in oxide formation with the Mg^{2+}-exchanged smectite, no corresponding increase in the oxide reduction peaks III′ or III was found, possibly because these oxides were dissolved by the smectite prior to the return sweep. A test to see whether increasing the scan rate (thus decreasing the contact time between the smectite and Fe oxides) would result in larger reduction peaks would be interesting.

Reductive dissolution. Reductive dissolution has been used to explain the dissolution of passive films in borate buffer at the OCP (Bardwell *et al.*, 1988; Deng *et al.*, 2004, 2006). In such a mechanism, the outer layers of the passive film are reduced by electrons that result from the oxidation of the Fe metal. Dissolution by this mechanism depends on film thickness as well as on whether the films have undergone reconstruction, which prevents short-circuit diffusion and only allows slower lattice diffusion (Deng *et al.*, 2004, 2006). The mechanism is probably not important during the evaporation of the smectite suspension on the Fe electrode, given the acidic nature of the dehydrated smectites and the likelihood that the passive films on the electrodes underwent reconstruction due to their exposure to air. The mechanism, however, may be more important in removing the hydroxide film formed at the active-passive transition in solution.

Sorption of Fe^{2+}

The acidic nature of the smectite does not completely explain the changes that were observed in the Fe electrode CV when a smectite coating was applied. When a CV is taken of an Fe electrode in borate buffer with a pH <8.4, the height of peak I increases significantly because of an increase in the rate of Fe dissolution (Diez-Perez *et al.*, 2001), just as was seen when a smectite coating was applied to the Fe electrodes (Figure 4). However, in an acidic electrolyte, the heights of peaks II′/II and III′/III also increase because more Fe(II) is produced, oxidized, and then reduced (Diez-Perez *et al.*, 2001).

While the CMIE CVs (Figure 4) showed a significant increase in peak I relative to the uncoated Fe electrodes, no corresponding increase in peaks II′/II or III′/III was observed. Note that a slight increase in peak III′ (relative to the reduced Fe electrode) was found but the reduction peak remained less prominent than expected relative to the height of peak I. Moreover, a shift in the position of peak I that would be expected if the CV were run in a lower pH solution was not observed. For example, when the CV for an Fe electrode in a borate buffer was recorded, peak I shifted anodically by ~0.1 V when the pH was decreased from 8.4 to 7.5 (Diez-Perez *et al.*, 2001). For the CMIE CVs, Peak I did not show an anodic shift; peak III/III′ was anodic of the corresponding peak for the uncoated Fe electrode but this was attributed to differences in the oxide that forms.

The changes in the CV observed when an Fe electrode is coated with smectite appear more similar to the changes that occur in the CV of Fe electrodes when compounds capable of chelating or complexing with Fe^{2+} are added to the borate buffer solution (Babić *et al.*, 2003; Liu and Macdonald, 2001; Modiano *et al.*, 2004; Rubim, 1993; Sikora and Macdonald, 2000). Typically, when an Fe^{2+} chelator was added to borate buffer, peak I increased, indicating an increased rate of corrosion, while peaks II′/II and III′/III decreased as less Fe^{2+} was available at the Fe surface to form Fe oxides because it complexed with the chelator. In the CMIE system, the smectite itself can act as a chelator. The Fe^{2+} can sorb at two different sites on the smectite surfaces: at the basal plane, adsorption occurs by an outer-sphere cation-exchange type mechanism; at the edges of the smectite layers, hydroxyl groups could form an inner-sphere surface complex with the Fe cation (Schultz and Grundl, 2004; Schultz and Grundl, 2000). Thus, while the smectite cannot form a soluble complex with Fe^{2+} that removes the ion from the Fe surface as a soluble compound like EDTA does, its ability to sorb the Fe^{2+} effectively removes this cation from the Fe surface, preventing it from becoming part of an oxide film that would later appear as a reduction peak in the CV. This adsorption mechanism is probably most important when the Fe is actively corroding and producing Fe^{2+} (under

https://doi.org/10.1346/CCMN.2012.0600204 Published online by Cambridge University Press

anodic bias or even at the OCP); when the Fe is passivated, the acidic nature of the smectite is more likely to be responsible for the dissolution of the passive layer. The sorption of Fe^{2+} by the smectite may at least partly explain why few oxides remained on the Fe surface when the smectite was biased at the active-passive transition potential prior to the CV scan.

Correlation between electrochemical behavior and smectite type

Except for E_{CORR}, the corrosion parameters obtained from the PPSs and the activity of the Fe (estimated from the relative height of peak I in the CVs) showed no significant dependence on smectite type within the experimental uncertainty. The trend in E_{CORR} and the height of peak I in the CV, however, was intriguing, suggesting that the electrodes coated with SAz-1 were less passivated/more active than electrodes coated with SWy-1 or SHCa-1. The smectite properties (Table 2) for which SAz-1 is at one extreme and SWy-1 and SHCa-1 at the other are CEC, surface area as measured by BET analysis, which does not include the internal surface associated with the interlayer region, and perhaps initial pH, although insufficient data were available for this last property. The dependence on smectite type is consistent with both the acidity of the smectite and its ability to sorb Fe^{2+} produced during the corrosion of the Fe being responsible for the effect that the presence of the smectite has on the electrochemical behavior of the underlying Fe electrode. The most acidic smectite would be expected to be most effective at removing Fe oxides at the surface of the electrode. The CEC might be expected to correlate with the acidity of the smectite as the protons donated are from water associated with the exchange cations. The surface area of the smectite may be related to the ability of the smectite to sorb Fe^{2+}. A complex interplay between many of the smectite properties exists, however, making it unlikely that this simple interpretation is complete and may be why significant differences in electrochemical behavior could not be found despite the range in values of the various clay properties. For example, the exchange cations may affect the electrochemical behavior because of their ability to polarize water as well as the possibility that they may exchange with the Fe^{2+} produced by the oxidation of the underlying Fe; also, sorption of Fe^{2+} on the smectite surface will be complicated by the possibility of electron transfer to structural Fe(III).

CONCLUSIONS

The PPSs and CVs taken with CMIEs and uncoated Fe electrodes suggest that the smectite removed the air-formed passive film originally present on the Fe electrodes during the coating process and prevented or limited growth of a passive film when the Fe electrode was biased anodically. Oxides that did form on the surface of the Fe in the presence of the smectite seemed to be different from those that formed on the surface of an uncoated Fe electrode. The Brønsted acidity of the smectite was probably responsible for the removal of the passive layer during the evaporation step of the CMIE preparation and to some degree when the CMIE was biased anodically. The ability of the smectite to sorb the Fe^{2+} produced when the Fe was actively corroding was probably most important in limiting the growth of a passive layer when the electrode was biased anodically. The presence of the smectite appeared to affect the composition of oxides that did form. This could be through the sorption of Fe^{2+} or through chemical reactions between the smectite and oxides.

The present study has suggested smectite properties, as well as techniques for combining the Fe and smectite, that should be considered when attempting to improve the efficiency of Fe-based permeable reactive barriers for remediation of contaminated groundwater. Under the right conditions, contact with smectites could remove oxides from already passivated Fe particles and limit growth of an oxide layer that may occur as the barriers age. The more acidic the smectite, the easier the removal of the passive layer and/or the prevention of the growth of oxides. More acidic smectites (*e.g.* those with more highly charged exchange cations or dehydrated smectites) should make the underlying Fe more active. The greater the ability of the smectite to sorb the Fe^{2+} produced as the Fe corrodes, the more active the Fe should remain as the system ages. This could be controlled by choosing smectites with larger CECs and/or surface areas.

An important question is how to obtain the necessary intimate contact between the smectite and ZVI particles to allow the protons of the smectite to dissolve the passive layer and/or the smectite to sorb Fe^{2+} ions. Evaporating a smectite suspension onto the Fe particles would be ideal; simply mixing smectite into an Fe wall slurry would probably fail. That smectite coating has the potential to act as a barrier between the Fe and groundwater contaminants is also relevant. Mechanisms exist, however, that might allow the contaminant to get through the smectite; the properties of the contaminants and smectite, however, will significantly affect the rate of transport through the smectite film and should also be kept in mind. Diffusion of solutes through smectite films has been studied and the rate of diffusion determined by the degree and type of smectite–solute interactions possible (Joo and Fitch, 1996; Subramanian and Fitch, 1992). Channels may develop through the smectite that allow the contaminant access to the Fe (Bard and Mallouk, 1992) or a contaminant could be indirectly reduced by the Fe as electron transfer or hopping may also occur by transfer between various species in the smectite film (Bard and Mallouk, 1992).

Finally, the work described here has implications for several recent studies looking at using smectite supports

https://doi.org/10.1346/CCMN.2012.0600204 Published online by Cambridge University Press

to prevent the aggregation of Fe nanoparticles used to remediate groundwater contaminants (Frost *et al.*, 2009; Gu *et al.*, 2010; Jia *et al.*, 2011; Katsenovich and Miralles-Wilhelm, 2009; Li *et al.*, 2010). In all cases, the smectite-supported nano-sized ZVI was more active than unsupported ZVI, and this was attributed to the ability of the smectites to keep the Fe nanoparticles dispersed. However, the results described here suggest that the effect that the smectite has on the composition of the oxide layer on these nanoparticles may play some role and should also be considered.

ACKNOWLEDGMENTS

The American Chemical Society Petroleum Research Fund is acknowledged for partial support of this research (ACS PRF# 38532-B 5). The smectite processing and initial experiments were conducted in the William R. Wiley Environmental Molecular Sciences Laboratory (EMSL), a U.S. Department of Energy (DOE) User Facility operated by Battelle for the DOE Office of Biological and Environmental Research. Pacific Northwest National Laboratory (PNNL) is operated for the DOE under Contract DE-AC06-76RLO 1830. The authors also acknowledge the loan of an EG&G Princeton Applied Research model 273A potentiostat from the EMSL. Funding for student support is gratefully acknowledged from Lewis & Clark College's John S. Rogers Summer Research program. Finally, the authors thank Jim Nurmi and Paul Tratnyek for their helpful comments and suggestions on the manuscript.

REFERENCES

Adams, J.M., Clapp, T.V., and Clement, D.E. (1983) Catalysis by montmorillonites. *Clay Minerals*, **18**, 411–421.

Agrawal, A. and Tratnyek, P.G. (1996) Reduction of nitro aromatic compounds by zero-valent iron metal. *Environmental Science & Technology*, **30**, 153–160.

Amonette, J.E. (2002) Iron redox chemistry of clays and oxides: environmental applications. Pp. 89–147 in: *Electrochemical Properties of Clays* (A. Fitch, editor). Workshop Lecture Series **10**, The Clay Minerals Society, Aurora, Colorado, USA.

Amonette, J.E., Camacho, E.A., and Divanfard, H.A. (1996) Reduction of chlorinated hydrocarbons by Fe(II)-bearing smectite. *33rd Annual Meeting, The Clay Minerals Society*, Gatlinburg, Tennessee, USA.

Babić, R., Metikoš-Huković, M., and Pilić, Z. (2003) Passivity of mild steel in borate buffer solution containing tannin. *Corrosion*, **59**, 890–896.

Bard, A.J. and Mallouk, T. (1992) Electrodes modified with clays, zeolites, and related microporous solids. Pp. 427 in: *Molecular Design of Electrode Surfaces* (R.W. Murray, editor). John Wiley & Sons, Inc.

Bardwell, J.A., MacDougall, B., and Graham, M.J. (1988) Use of ^{18}O/SIMS and electrochemical techniques to study the reduction and breakdown of passive oxide films on iron. *Journal of the Electrochemical Society*, **135**, 413–418.

Büchler, M., Schmuki, P., and Böhni, H. (1998) Iron passivity in borate buffer: formation of a deposit layer and its influence on the semiconducting properties. *Journal of the Electrochemical Society*, **145**, 609–614.

Carlson, L., Karnland, O., Oversby, V.M., Rance, A.P., Smart, N.R., Snellman, M., Vähänen, M., and Werme, L.O. (2007) Experimental studies of the interactions between anaerobically corroding iron and bentonite. *Physics and Chemistry of the Earth*, **32**, 334–345.

Cervini-Silva, J., Wu, J., Larson, R.A., and Stucki, J.W. (2000) Transformation of chloropicrin in the presence of iron-bearing clay minerals. *Environmental Science & Technology*, **34**, 915–917.

Cervini-Silva, J., Larson, R.A., Wu, J., and Stucki, J.W. (2001) Transformation of chlorinated aliphatic compounds by ferruginous smectite. *Environmental Science & Technology*, **35**, 805–809.

Cervini-Silva, J., Larson, R.A., Wu, J., and Stucki, J.W. (2002) Dechlorination of pentachloroethane by commercial Fe and ferruginous smectite. *Chemosphere*, **47**, 971–976.

Cervini-Silva, J., Kostka, J.E., Larson, R.A., Stucki, J.W., and Wu, J. (2003) Dehydrochlorination of 1,1,1-trichloroethane and pentachloroethane by microbially reduced ferruginous smectite. *Environmental Toxicology and Chemistry*, **22**, 1046–1050.

Deng, H., Ishikawa, I., Yoneya, M., and Nanjo, H. (2004) Reconstruction in air of an iron passive film formed at −0.4 V in a borate buffer solution. *Journal of Physical Chemistry B*, **108**, 9139–9146.

Deng, H., Nanjo, H., Qian, P., Xia, Z., and Ishikawa, I. (2006) Evolution of passivity in air exposure of an iron passive film. *Electrochimica Acta*, **52**, 187–193.

Diez-Perez, I., Gorostiza, P., Sanz, F., and Muller, C. (2001) First stages of electrochemical growth of the passive film on iron. *Journal of the Electrochemical Society*, **148**, B307–B313.

Féron, D., Crusset, D., and Gras, J.M. (2008) Corrosion issues in nuclear waste disposal. *Journal of Nuclear Materials*, **379**, 16–23.

Fitch, A. (1990) Clay-modified electrodes: A review. *Clays and Clay Minerals*, **38**, 391–400.

Frenkel, M. (1974) Surface acidity of montmorillonites. *Clays and Clay Minerals*, **22**, 435–441.

Frost, R.L., Xi, Y., and He, H. (2009) Synthesis, characterization of palygorskite supported zero-valent iron and its application for methylene blue adsorption. *Journal of Colloid and Interface Science*, **341**, 153–161.

Gibbs, M.M. (1979) A simple method for the rapid determination of iron in natural waters. *Water Research*, **13**, 295–297.

Gillham, R.W. and O'Hannesin, S.F. (1994) Enhanced degradation of halogenated aliphatics by zero-valent iron. *Ground Water*, **32**, 958–967.

Gu, B., Liang, L., Dickey, M.J., Yin, X., and Dai, S. (1998) Reductive precipitation of uranium(VI) by zero-valent iron. *Environmental Science & Technology*, **32**, 3366–3373.

Gu, C., Jia, H., Li, H., Teppen, B.J., and Boyd, S.A. (2010) Synthesis of highly reactive subnano-sized zero-valent iron using smectite clay templates. *Environmental Science & Technology*, **44**, 4258–4263.

Hofstetter, T.B., Schwarzenbach, R.P., and Haderlein, S.B. (2003) Reactivity of Fe(II) species associated with clay minerals. *Environmental Science & Technology*, **37**, 519–528.

Hofstetter, T.B., Neumann, A., and Schwarzenbach, R. (2006) Reduction of nitroaromatic compounds by Fe(II) species associated with iron-rich smectites *Environmental Science & Technology*, **40**, 235–242.

Ilton, E.S., Heald, S.M., Smith, S.C., Elbert, D., and Liu, C. (2006) Reduction of uranyl in the interlayer region of low iron micas under anoxic and aerobic conditions. *Environmental Science & Technology*, **40**, 5003–5009.

Jackson, M.L. (1979) *Soil Chemistry Analysis – Advanced Course*. Published by the author, Madison, Wisconsin, USA.

Jackson, M.L., Whittig, L.D., and Pennington, R.P. (1950) Segregation procedure for the mineralogical analysis of soils. *Soil Science Society of America Proceedings*, **14**, 77–81.

Jaisi, D.P., Dong, H., Plymale, A.E., Fredrickson, J.K., Zachara, J.M., Heald, S., and Liu, C. (2009) Reduction and long-term immobilization of technetium by Fe(II) associated with clay mineral nontronite. *Chemical Geology*, **264**, 127–138.

Jensen, W.B. (2008) The origin of the rubber policeman. *Journal of Chemical Education*, **85**, 776.

Jia, H., Gu, C., Boyd, S.A., Teppen, B.J., Johnston, C.T., Song, C., and Li, H. (2011) Comparison of reactivity of nanoscaled zero-valent iron formed on clay surfaces. *Soil Science Society of America Journal*, **75**, 357–364.

Johnson, T.L., Scherer, M.M., and Tratnyek, P.G. (1996) Kinetics of halogenated organic compound degradation by iron metal. *Environmental Science & Technology*, **30**, 2634–2640.

Joo, P. and Fitch, A. (1996) Ionic and molecular transport in hydrophobized montmorilllonite films: An electrochemical survey. *Environmental Science & Technology*, **30**, 2681–2686.

Jovancicevic, V., Kainthla, R.C., Tang, Z., Yang, B., and Bockris, J.O.M. (1987) The passive film on iron: an ellipsometric-spectroscopic study. *Langmuir*, **3**, 388–395.

Katsenovich, Y. and Miralles-Wilhelm, F.R. (2009) Evaluation of nanoscale zerovalent iron particles for trichloroethene degradation in clayey soils. *Science of the Total Environment*, **407**, 4986–4993.

Klausen, J., Vikesland, P.J., Kohn, T., Burris, D.R., Ball, W.P., and Roberts, A.L. (2003) Longevity of granular iron in groundwater treatment processes: Solution composition effects on reduction of organohalides and nitroaromatic compounds. *Environmental Science & Technology*, **37**, 1208–1218.

Kohn, T., Kane, S.R., Fairbrother, D.H., and Roberts, A.L. (2003) Investigation of the inhibitory effect of silica on the degradation of 1,1,1-trichloroethane by granular iron. *Environmental Science & Technology*, **37**, 5806–5812.

Kohn, T., Livi, J.T., Roberts, A.L., and Vikesland, P.J. (2005) Longevity of granular iron in groundwater treatment processes: Corrosion product development. *Environmental Science & Technology*, **39**, 2867–2879.

Krishnamurti, G.S.R., Violante, A., and Huang, P.M. (1998) Influence of montmorillonite on Fe(II) oxidation products. *Clay Minerals*, **33**, 205–212.

Lear, P.R. and Stucki, J.W. (1989) Effects of iron oxidation state on the specific surface area of nontronite. *Clays and Clay Minerals*, **37**, 547–552.

Lee, H.-J., Chun, B.-S., Kim, W.-C., Chung, M., and Park, J.-W. (2006) Zero valent iron and clay mixtures for removal of trichloroethylene, chromium(VI), and nitrate. *Environmental Technology*, **27**, 299–306.

Li, S., Wu, P., Li, H., Zhu, N., Li, P., Wu, J., Wang, X., and Dang, Z. (2010) Synthesis and chararacterization of organo-montmorillonite supported iron nanoparticles. *Applied Clay Science*, **50**, 330–336.

Liu, J. and Macdonald, D.D. (2001) The passivity of iron in the presence of ethylenediaminetetraacetic acid: II. The defect and electronic structures of the barrier layer. *Journal of the Electrochemical Society*, **148**, B425–B430.

Madsen, F.T. (1998) Clay mineralogical investigations related to nuclear waste disposal. *Clay Minerals*, **33**, 109–129.

Matheson, L.J. and Tratnyek, P.G. (1994) Reductive dehalogenation of chlorinated methanes by iron metal. *Environmental Science & Technology*, **28**, 2045–2053.

Merola, R.B., Fournier, E.D., and McGuire, M.M. (2007) Spectroscopic investigations of Fe^{2+} complexation on nontronite clay. *Langmuir*, **23**, 1223–1226.

Modiano, S., Fugivara, C.S., and Benedetti, A.V. (2004) Effect of citrate ions on the electrochemical behavior of low-carbon steel in borate buffer solutions. *Corrosion Science*, **46**, 529–545.

Mortland, M.M. and Raman, K.V. (1968) Surface acidity of smectites in relation to hydration, exchangeable cation, and structure. *Clays and Clay Minerals*, **16**, 393–398.

Neumann, A., Hofstetter, T.B., Lüssi, M., Cirpka, O.A., Petit, S., and Schwarzenbach, R. (2008a) Assessing the redox reactivity of structural iron in smectites using nitroaromatic compounds as kinetic probes. *Environmental Science & Technology*, **42**, 8381–8387.

Neumann, A., Hofstetter, T.B., Lüssi, M., Cirpka, O.A., Petit, S., and Schwarzenbach, R.P. (2008b) Assessing the redox reactivity of structural iron in smectities using nitroaromatic compounds as kinetic probes. *Environmental Science & Technology*, **42**, 8381–8387.

Neumann, A., Hofstetter, T.B., Skarpeli-Liati, M., and Schwarzenbach, R.P. (2009) Reduction of polychlorinated ethanes and carbon tetrachloride by structural Fe(II) in smectites. *Environmental Science & Technology*, **43**, 4082–4089.

Neumann, A., Sander, M., and Hofstetter, T.B. (2012) Redox properties of structural Fe in clay minerals. Pp. 361–379 in: *Aquatic Redox Chemistry* (P.G. Tratnyek, T.J. Grundl, and S.B. Haderlein, editors). ACS Symposium Series, **1071**, The American Chemical Society, Washington, D.C.

Nurmi, J.T., Bandstra, J.Z., and and Tratnyek, P.G. (2004) Packed powder electrodes for characterizing the reactivity of granular iron in borate solutions. *Journal of the Electrochemical Society*, **151**, B347–B353.

Nurmi, J.T., Tratnyek, P.G., Sarathy, V., Baer, D.R., Amonette, J.E., Pecher, K., Wang, C., Linehan, J.C., Matson, D.W. Penn, R.L., and Driessen, M.D. (2005) Characterization and properties of metallic iron nanoparticles: Spectroscopy, electrochemistry, and kinetics. *Environmental Science & Technology*, **39**, 1221–1230.

Nzengung, V.A., Castillo, R.M., Gates, W.P., and Mills, G.L. (2001) Abiotic transformation of perchloroethylene in homogeneous dithionite solution and in suspensions of dithionite-treated clay minerals. *Environmental Science & Technology*, **35**, 2244–2251.

Oblonsky, L.J. and Devine, T.M. (1995) A surface enhanced Raman spectroscopic study of the passive films formed in borate buffer on iron, nickel, chromium and stainless steel. *Corrosion Science*, **37**, 17–41.

Oh, Y.J., Song, H., Shin, S.S., Choi, S.J., and Kim, Y.-H. (2007) Effect of amorphous silica and silica sand on removal of chromium(VI) by zero-valent iron. *Chemosphere*, **66**, 858–865.

Olphen, H.V. and Fripiat, J.J. (1979) *Data Handbook for Clay Materials and Other Non-Metallic Minerals*. Pergamon Press, New York.

Peretyazhko, T., Zachara, J.M., Heald, S.M., Jeon, B.-H., Kukkadapu, R.K., Liu, C., Moore, D., and Resch, C.T. (2009) Heterogeneous reduction of Tc(VII) by Fe(II) at the solid-water interface. *Geochimica et Cosmochimica Acta*, **72**, 1521–1539.

Powell, R.M. and Puls, R.W. (1997) Proton generation by dissolution of intrinsic or augmented aluminosilicate minerals for in situ contaminant remediation by zero-valence-state iron. *Environmental Science & Technology*, **31**, 2244-2251.

Powell, R.M., Puls, R.W., Hightower, S.K., and Sabatini, D.A. (1995) Coupled iron corrosion and chromate reduction: Mechanisms for subsurface remediation. *Environmental Science & Technology*, **29**, 1913–1922.

Rabideau, A.J., Shen, P., and Khandelwal, A. (1999) Feasibility of amending slurry walls with zero-valent iron. *Journal of Geotechnical and Geoenvironmental Engineering*, **April**, 330–333.

Research, E.G.P.A. (1987) Electrochemistry and Corrosion: Overview and Techniques. *Application Note*, **Corr-4**, 1–16.

Reynolds, G.W., Hoff, J.T., and Gillham, R.W. (1990) Sampling bias caused by materials used to monitor halocarbons in groundwater. *Environmental Science & Technology*, **24**, 135–142.

Roberts, A.L., Totten, L.A., Arnold, W.A., Burris, D.R., and Campbell, T.J. (1996) Reductive elimination of chlorinated ethylenes by zero-valent metals. *Environmental Science & Technology*, **30**, 2654–2659.

Rodriguez, E.A., Amonette, J.E., Divanfard, H.R., and Marquez, J.F. (1999) Use of Fe(II) associated with layer silicates for remediation of groundwater contaminated by CCl_4, TCE and TNT. Pp. 41–42 in: *Environmental Molecular Sciences Symposia and First User's Meeting*. Abstracts with Program, Pacific Northwest National Laboratory, Washington, USA.

Rubim, J.C. (1993) *In situ* raman and reflectance spectra of iron electrodes in borate buffer solution containing 2,2'-bipyridine. *Journal of the Electrochemical Society*, **140**, 1601–1606.

Sawyer, D.T., Sobkowiak, A., and Roberts, J.L. (1995) *Electrochemistry for Chemists*. John Wiley & Sons, Inc., New York.

Schaefer, M.V., Gorski, C.A., and Scherer, M.M. (2011) Spectroscopic evidence for interfacial Fe(II)–Fe(III) electron transfer in a clay mineral. *Environmental Science & Technology*, **45**, 540–545.

Scherer, M.M., Westall, J.C., Ziomek-Moroz, M., and Tratnyek, P.G. (1997) Kinetics of carbon tetrachloride reduction at an oxide-free iron electrode. *Environmental Science & Technology*, **31**, 2385–2391.

Schultz, C.A. and Grundl, T.J. (2000) pH dependence on reduction rate of 4-Cl-nitrobenzene by Fe(II)/montmorillonite systems. *Environmental Science & Technology*, **34**, 3641–3648.

Schultz, C. and Grundl, T. (2004) pH dependence of ferrous sorption onto two smectite clays. *Chemosphere*, **57**, 1301–1306.

Sikora, E. and Macdonald, D.D. (2000) The passivity of iron in the presence of ethylenediaminetetraacetic acid: I. General electrochemical behavior. *Journal of the Electrochemical Society*, **147**, 4087–4092.

Smart, N.R., Rance, A.P., and Werme, L.O. (2004) Anaerobic corrosion of steel in bentonite. *Materials Research Society Symposium Proceedings*, **807**, 441–446.

Soma, Y. and Soma, M. (1989) Chemical reactions of organic compounds on clay surfaces. *Environmental Health Perspectives*, **83**, 205–214.

Source Clay Physical/Chemical Data http://www.agry.purdue.edu/cjohnston/sourceclays/chem.htm (February 21, 2012).

Stookey, L.L. (1970) Ferrozine – a new spectrophotometric reagent for iron. *Analytical Chemistry*, **42**, 779–781.

Subramanian, P. and Fitch, A. (1992) Diffusional transport of solutes through clay: use of clay-modified electrodes. *Environmental Science & Technology*, **26**, 1775–1779.

Tanner, C.B. and Jackson, M.L. (1948) Nomographs of sedimentation times for soil particles under gravity or centrifugal acceleration. *Soil Science Society of America Proceedings*, **12**, 60–65.

Thompson, D.W. and Mitchell, C.J. (1993) The hydrolytic precipitation of iron in aqueous dispersions of mineral particles. *Colloids and Surfaces A: Physicochemical and Engineering Aspects*, **73**, 103–115.

Tratnyek, P.G. (1996) Putting corrosion to use: Remediation of contaminated groundwater with zero-valent metals. *Chemical Industry (London)*, 499–503.

Vela, M.W., Vilche, J.R., and Arvia, A.J. (1986) The dissolution and passivation of polycrystalline iron electrodes in boric acid-borate buffer solutions in the 7.5–9.2 pH range. *Journal of Applied Electrochemistry*, **16**, 490–504.

Virtanen, S., Schmuki, P., Davenport, A.J., and Vitus, C., M. (1997) Dissolution of thin iron oxide films used as models for iron passive films studied by in situ X-ray absorption near-edge spectroscopy. *Journal of the Electrochemical Society*, **144**, 198–204.

Wei, J., Furrer, G., Kaufmann, S., and Schulin, R. (2001) Influence of clay minerals on the hydrolysis of carbamate pesticides. *Environmental Science & Technology*, **35**, 2226–2232.

Zen, J.-M., Jeng, S.-H., and Chen, H.-J. (1996) Catalysis of the electroreduction of hydrogen peroxide by nontronite clay coatings on glassy carbon electrodes. *Journal of Electroanalytical Chemistry*, **408**, 157–163.

(*Received 12 October 2011; revised 28 March 2012; Ms. 623; A.E. H. Dong*)